Research Square

Preprints are preliminary reports that have not undergone peer review.
They should not be considered conclusive, used to inform clinical practice,
or referenced by the media as validated information.

Biosynthesis of Silver Nanoparticles using Barley straw and Fumaria parviflora extract: Optimization of synthesis, Evaluating of Nanoparticles stability, Antibacterial activities

Maryam Fakharzadeh (mfakharzadeh@tvu.ac.ir)
Technical and Vocational University

Seyed Esmail Fazljoo
Technical and Vocational University

Research Article

Keywords: Biosynthesis, Silver Nanoparticles, Barley straw, Fumaria parviflora, Nanoparticles stability, Antibacterial activity

Posted Date: April 20th, 2023

DOI: https://doi.org/10.21203/rs.3.rs-2800656/v1

License: This work is licensed under a Creative Commons Attribution 4.0 International License.
Read Full License

Additional Declarations: No competing interests reported.

Version of Record: A version of this preprint was published at BioNanoScience on November 14th, 2023. See the published version at https://doi.org/10.1007/s12668-023-01242-7.

Abstract

This study indicates an environmentally friendly and cost-effective method for the biosynthesis of silver nanoparticles using *Barley straw* and *Fumaria paroflora* extracts and a mixture of them (1:1 v/v). Optimum conditions for the synthesis of silver nanoparticles were obtained by changing the reaction time, PH, and temperature. Characterization of silver nanoparticles was explored by different techniques including UV-Visible spectroscopy, FTIR, X-ray diffraction, and SEM. UV-Visible spectroscopy showed the formation of *Bs-AgNPs*, *Fp-AgNPs*, and *Bs-Fp-AgNPs* with maximum absorption in the range of 400–450 nm. FTIR spectral data revealed the role of different functional groups of biomolecules involved in bioreduction as well as the capping and stabilizing of NPs. XRD analysis confirmed the formation of silver nanoparticles. The SEM study showed that the shape of the nanoparticles is spherical, and the size decreases with increasing temperature. The size and surface charge of nanoparticles were evaluated by dynamic light scattering (DLS) spectroscopy, and the effect of temperature on particle size distribution was evaluated. Also, the effect of temperature and PH on the zeta potential of nanoparticles was investigated. The formation rate of *Fp-AgNPs* was higher compared to *Bs-AgNPs*, but *Barley straw* nanoparticles were smaller and more stable. Using a mixture of *Fumaria parviflora* and *Barley straw* extract resulted in the production of nanoparticles that formed faster and had good stability. The biosynthesized nanoparticles showed suitable activity against *Escherichia coli* and *Staphylococcus aureus*. Overall, this study highlights the use of a mixture of extracts (Bs and Fp) to synthesize silver nanoparticles.

1 Introduction

Nanotechnology is growing and developing rapidly due to its wide scope in science and industry. The range of applications of this technology in chemistry, physics, medicine, and electronics is so much that it has caused a great scientific revolution in the world [1]. Scientific nanotechnology is based on nanoparticles; particles with a three-dimensional structure are stable with a size between 1 to 100 nm. These have unique mechanical, optical, electrical, thermal, chemical, and magnetic properties due to their minimal size and high surface-to-volume ratio [2]. There are various processes, including chemical and physical methods, for the synthesis of nanoparticles of different sizes [3]. Many of these methods are expensive and time-consuming and require various hazardous chemicals to synthesize and stabilize nanoparticles, leading to the production of byproducts incompatible with the environment [4]. Considering the significant problems that exist in chemical and physical methods for the production of nanoparticles, there is a need to develop biological methods compatible with the environment, affordable, and free of harmful chemicals. The use of microorganisms and plant extracts can be suitable method for the synthesis of silver nanoparticles [5]. The synthesis of nanoparticles using biological materials has become the interest of many researchers due to their new chemical and physical properties and many applications in various medical, agricultural, optical, electronical, and mechanical sciences [6]. These particles show specific physical and chemical properties and biological activities. Several theories have been proposed to explain the antimicrobial effect of silver nanoparticles. Silver nanoparticles attach to

the cell wall and penetrate it, which causes structural damage to the cell wall and bacterial membrane [7, 8]. Plants can be widely used due to their compatibility with the environment without causing environmental damage [9]. Studies indicate that plants, as rich sources of antimicrobial compounds, contain significant amounts of biological molecules such as amino acids, enzymes, alkaloids, tannins, phenolics, saponins, carbohydrates, flavonoids, volatile oils, and vitamins [10, 11]. For this reason, the use of a wide group of plants, especially medicinal plants, has attracted the attention of researchers.

Silver nanoparticles synthesized by the biological method have outstanding features such as high surface area, high dispersion, and small size. The combination of these factors causes the antimicrobial effects of silver nanoparticles significantly increase compared to silver [12]. Silver nanoparticles (AgNPs) have become one of the commercially available nanoparticles due to their wide applications in industry and daily life.

In this research, the green synthesis of silver nanoparticles using the aqueous extract of *Fumaria parviflora* (Fp) and *Barley straw* (Bs) and the antibacterial properties of the synthesized nanoparticles were investigated. Also, the effect of the mixture of two aqueous extracts of *Fumaria parviflora* and *Barley straw* in synthesizing silver nanoparticles and the antibacterial properties of the resulting nanoparticles were investigated. Phytochemical studies showed that *Fumaria parviflora* contains more Flavonoids, glycosides, tannins, saponins, Steroids, triterpenoids, phenols, alkaloids, and Anthraquinones [13], and the main constituents of *Barley straw* include cellulose, hemicellulose, lignin, and inorganic minerals [14]. Affordability, availability, and Significant pharmacological effects of *Fumaria parviflora* (Fp) and *Barley straw* (Bs) are the main advantages of using these plants for silver ion reduction. This research provides data on the synthesis of silver nanoparticles using the aqueous extract of *Fumaria parviflora* (Fp) and *Barley straw* (Bs) as well as the mixture of *Fumaria parviflora* and *Barley straw* extracts and investigating their antibacterial properties. Based on this, the main contribution of the present study can be considered as follows:

1. Utilization of *Fumaria parviflora* (Fp) extracts as green stabilizing and reducing agents
2. Utilization of *Barley straw* (Bs) extracts as green stabilizing and reducing agents
3. Using a mixture of *Fumaria parviflora* (Fp) and *Barley straw* (Bs) extracts as stabilizing and reducing agents.
4. Optimization of synthesis silver nanoparticles
5. Investigation of silver nanoparticles prepared in parts 1, 2, and 3 by various techniques such as UV/Vis spectroscopy, FTIR, XRD, SEM–EDX, and DLS.
6. Examining the antibacterial activity of nanoparticles obtained in parts 1, 2, and 3 against *Staphylococcus aureus* and *Escherichia coli.*

2 Materials And Methods

2.1 Plant Extracts

Fumaria parviflora (Fp) and *Barley straw* (Bs) were supplied from the herbarium of the medicinal plants of Isfahan University of Technology. To prepare extracts of *Fumaria parviflora* (Fp) and *Barley straw* (Bs), 5 grams of each plant were boiled in 100 mL of distilled water at 80°C for 20 minutes to obtain the bioactive compounds. The extracts were filtered using Whatman No.1 filter paper and stored at 4°C for the synthesis of silver nanoparticles. Also, the effect of the mixture of aqueous extracts of *Barley straw* and *Fumaria parviflora* (1:1 v/v) on the synthesis of silver nanoparticles was evaluated.

2.2 Synthesis of Silver Nanoparticles

To provide Fp-AgNPs, Bs-AgNPs, and Fp-Bs-AgNPs, 5mL of *Fumaria parviflora* (Fp), *Barley straw* (Bs) extracts, and a mixture of extracts (1:1 v/v) was added to 50mL of aqueous $AgNO_3$ solution (1Mm) for reduction of Ag^+ ions, separately. For the efficient synthesis of silver nanoparticles, the effect of reaction time, pH, and temperature on the formation of AgNPs was investigated, and the optimal conditions were selected for the reaction. The first sign of the reaction was determined by the color change. The suspensions of silver nanoparticles were centrifuged at 10,000 rpm for 10 min and the sediment was washed twice with 6 mL of distilled water. Finally, silver nanoparticles were dried in a vacuum oven at 40°C for 12 hours. The formation of silver nanoparticles using aqueous extracts Fp, Bs, and a mixture of extracts Fp and Bs (1:1 v/v) was investigated by UV/Vis (V-670/JASCO).

2.2.1 Effect of Reaction time

To evaluate the effect of reaction time on the synthesis of Fp-AgNPs, Bs-AgNPs, and Fp-Bs-AgNPs, at first, 5 ml of the desired extract was mixed with 50 ml of 1 mM silver nitrate at 25 °C, and after that the color of the solution changed, synthesized silver nanoparticles were monitored by UV/Vis (300–700 nm operated at a resolution of 1 nm) at specific time intervals.

2.2.2 Effect of pH

To provide Fp-AgNPs, Bs-AgNPs, and Fp-Bs-AgNPs, 5mL of each aqueous extract, was added to 50mL of aqueous $AgNO_3$ solution (1Mm) for reduction of Ag + ions separately. To adjust the pH of the reaction, HCl (0.1 M) and NaOH (0.1 M) were used. The effect of pH 4, 6, 8, 10, and 12 on the synthesis of silver nanoparticles was investigated, and silver nanoparticles synthesized were monitored by UV/Vis (300–700 nm operated at a resolution of 1 nm).

2.2.3 Effect of temperature

The effects of temperature on the synthesis of silver nanoparticles were studied by performing the reaction in a water bath at 25, 35, 45, 55, 65, and 75˚C. The pH of the reaction mixture was adjusted to 12 using 0.1 M NaOH.

5 ml of aqueous extract prepared of *Barley straw*, *Fumaria parviflora*, and a mixture of extracts (1:1 v/v) mixed with 50 ml of silver nitrate aqueous solution (1 mM) and the effect of temperature change on the

synthesis of silver nanoparticles was investigated and silver nanoparticles synthesized was monitored by UV/Vis (300–700 nm operated at a resolution of 1 nm).

2.3 Characterization of AgNPs

The green synthesis of AgNPs was analyzed using a UV-Vis spectrophotometer (UV-670/JASCO, Japan) to investigate the reduction of silver ions in 300–700 nm. FT-IR spectroscopic analysis was performed using (IR-6300/ JASCO, Japan) which was recorded in the range of 400–4000 cm^{-1} using a KBr pellet method to identify the functional groups. The XRD profile of AgNPs was evaluated by X-ray diffraction (Bruker D8ADVANCE, Germany) with Cu Kα radiation of 1.54178 Å at 40 kV and 30 mA in the range of 2Θ (20–90) degrees. The average hydrodynamic diameter (DLS) and stability of AgNPs were measured by a nanoparticle analyzer the SZ-100 HORIBA, Ltd. The morphology and the elemental composition of AgNPs were determined using (FE-SEM ZEISS Sigma 300, Germany), scanning electron microscopy (SEM) equipped with an energy-dispersive X-ray spectrometer (EDX).

2.4 Antibacterial activity

The standard disk diffusion method[15] was used to determine the bactericidal activity of Bs-AgNPs, Fp-AgNPs, Bs-Fp-AgNPs, and aqueous extracts against two pathogenic bacteria, *Escherichia coli* (ATCC 35218) as Gram-negative and *Staphylococcus aureus* (ATCC 29213) as Gram-positive. The commercial antibiotic disk containing amoxicillin (25 µg/disk) were selected as a positive control.

3 Results And Discussion

3.1 Optimization Study on the Biosynthesis of AgNPs

3.1.1 Effect of Reaction Time

Reaction time is an essential factor in the synthesis of silver nanoparticles. The reaction time means the time required for the reduction of silver ions and their conversion into silver nanoparticles. To investigate the effect of reaction time, pH = 12 and T = 25°C were kept constant. As shown in Fig. 1, the peak intensity gradually increased with time and reached a maximum of 180 min for Bs-AgNPs and 40 min for Fp-AgNPs, and 90 min for Fp-Bs-AgNP. No change in absorption was observed after 180 minutes for Bs-AgNPs, 40 minutes for Fp-AgNPs, and 90 minutes for Bs-Fp-AgNPs, which indicates the complete conversion of Ag + to Ag [16, 17]. Also, by increasing the reaction time, a blue shift is observed in the maximum absorption in the UV/Vis spectrum of Bs-AgNPs and Fp-AgNPs. But for the nanoparticles synthesized from the mixture of extracts, no change in the maximum wavelength was observed by increasing the reaction time. Figure 1 demonstrates that the absorption increase with contact time. UV-Vis absorption measurements were confirmed for silver nanoparticles in the range of 400–450 nm [18].

3.1.2 Effect of pH

The effect of pH on the formation of silver nanoparticles was evaluated using UV-vis. The formation of silver nanoparticles mainly depends on the pH of the reaction medium, and the intensity of surface plasmon resonance absorption bands increases with increasing pH range and reaches a maximum at pH = 12. (Fig. 2) In many biochemical and chemical processes, H^+ and OH^- ions have a significant effect. In the biosynthesis process of nanoparticles, the presence of OH^- ions has an activating effect and the presence of H^+ ions has an inhibitory effect. OH^- ions activate the functional groups in aqueous extracts and thus rapidly reduce silver ions [19]. As shown in Fig. 2, pH changes had the same effect on the synthesis of Bs-AgNPs, Fp-AgNPs, and Bs-Fp-AgNPs had the same effect, and no nanoparticles were formed at acidic pH. By increasing the pH of the reaction solution, the rate of formation of nanoparticles increases and reaches a maximum at pH = 12.

3.1.3 Effect of temperature

The effect of temperature on the synthesis of AgNPs was evaluated according to UV-Vis absorption peaks. As shown in Fig. 3, the absorption intensity increased with increasing temperature, indicating an increase in the production of silver nanoparticles. Also, a blue shift in the wavelength of the maximum in the UV-visible spectrum can be seen, which indicates the size reduction of produced nanoparticles with increasing temperature. These results are consistent with the results obtained in previous researchs [20, 21].

3.2 Characterization of the AgNPs

3.2.1 FTIR Spectroscopy Analysis

FTIR spectra were used to determine the chemical groups in AgNPs, identify possible biomolecules acting as reducing agents, and determine potential capping and stabilizing agents during the synthesis of AgNPs [22]. Many functional groups present that may be responsible for the reduction of Ag^+ ions. The intensity of the band in different regions was analyzed for plant extracts and silver nanoparticles and is shown in Fig. 4. Figure 4a showed the FTIR spectra of Bs aqueous extract and the final products of AgNPs; the FTIR spectrum of Bs extracts shows different major peak positions at 3398, 2926, 1625,1420,1102,786,601and 471 cm^{-1} and FTIR spectrum of Bs-AgNPs shows different major peak positions at 3412, 2925, 1603, 1420, 1088, 608, and 470 cm^{-1}. The broad and intense peak at (3398–3412) cm^{-1} corresponds to OH stretching vibrations of the phenol/carboxylic group present in the extract, and a peak at (2926 – 2925) cm^{-1} can be assigned to the stretching vibrations of the $-CH_2$ and $-CH_3$ functional groups. The peak at (1625 – 1603) cm^{-1} could be assigned to C = O stretching or amide bending [23]. Another peak at 1420 cm^{-1} confirmed the presence of C-C stretching of aromatic compounds. The band at (1102 – 1088) cm^{-1} for stretching vibrations of functional group C-O, and 786 cm^{-1} assigned to C-H alkenes stretch. The presence of alkyl halide stretching has been confirmed by the band of (601–608) cm^{-1}. Figure 4b showed the FTIR spectra of Fp aqueous extract and the final products of AgNPs, FTIR spectrum of Fp extracts shows different major peak positions at 3391, 2928, 1596,1418,1042, 618 cm^{-1}, and FTIR spectrum of Fp-AgNPs shows different major peak positions at

3409, 2920, 1592, 1384, 1031, and 557 cm^{-1}. The broad and intense peak in the (3391–3409) cm^{-1} corresponds to the OH stretching vibration of phenolic compounds, carboxylic acids, and alcohols [24]. The peaks (2928 – 2920) cm^{-1} can be considered stretching vibrations of the -CH_2 and -CH_3 functional groups. The existence of C = C and C = O groups has been confirmed as sharp peaks (1596 – 1592) cm^{-1} and can be related to the aromatic compounds and carbonyl groups [25]. The presence of C-C stretching of aromatic compounds was confirmed by another peak at (1418 – 1384) cm^{-1}. The peak located at (1042 – 1031) cm^{-1} is related to the C-O stretching, and the peaks in (618 – 557) cm^{-1} indicate the presence of halogen compounds and aromatic compounds [26]. The FTIR spectrum of plant extracts (Bs, Fp) and silver nanoparticles (Bs-AgNPs, Fp-AgNPs) shows a major change in OH groups, which indicates its dual role as a reducing and stabilizing agent [27, 28].

3.2.2 XRD Analysis

X-ray diffraction analyses were performed to confirm the crystalline structure and nanostructure of Bs-AgNPs and Fp-AgNPs. Several peaks were observed in the XRD pattern, at 2Θ = 28.10˚, 32.58 ˚, 38.42 ˚, 46.58 ˚, 65.06 ˚, 77.38 in Bs-AgNPs (Fig. 5a), which could be indexed to reflections (111), (200), (200), (220), (311), (420), indicating the presence of face-centered cubic (FCC) and crystalline structure of Bs-AgNPs. Similar results were obtained by recording Fp-AgNPs (Fig. 5b), peaks located at 2Θ = 27.18˚, 32.14 ˚, 38.03 ˚, 46.16 ˚, 64.58 ˚, 77.48 ˚, that could be indexed to (111), (200), (200), (220), (311), (420) reflections on the face-centered of crystalline Fp-AgNP cubic structure, (JCPDS, file No. 04-0783) [29]. The size of silver nanoparticles was determined by using the Scherrer equation ($D = K\lambda/\beta\cos\theta$) D: is the average size, λ: is the X-ray wavelength, K is a dimensionless shape factor(0.99), β: is the line broadening at half the maximum intensity (FWHM), and θ: is the Bragg angle. The calculated particle size of AgNPs using the Scherrer equation was equal to 19.81 nm for the Bs-AgNPs and 27.8 nm for the Fp-AgNPs are recorded in Tables 1 and 2.

Table 1
XRD analysis data using the Scherrer equation $D = K\lambda/\beta\cos\theta$ (Bs-AgNPs)

Peak Number	Peak position [°2θ]	FWHMβ [°]	Crystallite size [nm]	Average D [nm]
1	28.1	0.492	18.3	19.81
2	32.542	0.246	37	
3	38.315	0.59	15.7	
4	46.582	0.492	19.3	
5	54.946	0.295	33.4	
6	57.967	0.984	10.2	
7	65.056	0.787	13.2	
8	77.38	0.984	11.4	

Table 2
XRD analysis data using the Scherrer equation D = Kλ/βcosθ (Fp-AgNPs)

Peak Number	Peak position [°2θ]	FWHMβ [°]	Crystallite size [nm]	Average D [nm]
1	27.185	0.197	45.7	27.81
2	32.141	0.246	37	
3	38.028	0.295	31.3	
4	46.165	0.295	32.2	
5	54.647	0.59	16.7	
6	57.443	0.59	16.9	
7	64.581	0.344	30	
8	77.476	0.886	12.7	

3.2.3 SEM and EDX Analysis

SEM technique was used to determine the surface morphology and size of synthesized silver nanoparticles. Figure 6 shows the SEM image of Bs-AgNps, Fp-AgNPs, and Bs-Fp-AgNPs at 25 and 75°C. As could be seen in the figure, with the increase in temperature, the size of the synthesized nanoparticles decreased and the nanoparticles are mostly spherical. Temperature increases the rate of reduction, which leads to a decrease in reaction time. Therefore, increasing the temperature may lead to smaller AgNPs. An increase in temperature also increases the kinetic energy of molecules, which increases the use of silver ions [30, 31]. Similar observations were made by Rakib-Uz-Zaman, et al. [32].

Figure 7 displays the results of the EDX studies for Bs-AgNPs, Fp-AgNPs, and Bs-Fp-AgNPs. The presence of elemental silver was confirmed by the EDX signal at 3 keV. Additionally, Other elements, such as carbon and oxygen mainly, were also obtained in EDX analysis, which is attributed to the existence of phytochemicals in plant extracts that are linked to the surface of silver nanoparticles [25, 33]. Some other elements, such as Cd and Al, in the structure of silver nanoparticles, can be due to absorption from the soil, which can easily be integrated into the structure of nanoparticles [34, 35]. The presence of Au is related to sample preparation for analysis. A small drop of the aqueous solution of nanoparticles was placed on the glass slide and then air-dried and coated by sputtering with gold.

3.2.4 DLS and Zeta Potential Analysis

Dynamic light scattering (DLS) is a technique in physics that can be used to determine the hydrodynamic diameter of a nanoparticle and determine the distribution of particles in solutions and suspensions in the range of several nanometers to microns. Zeta potential determines the effective electric charge on the

surface of nanoparticles and is an important parameter to describe the stability in the aqueous suspension of nanoparticles. Also, the magnitude of zeta potential predicts the stability of nanoparticles [36, 37].

According to Fig. 8, the average size of the nanoparticle synthesized from Bs extract is smaller than the nanoparticle synthesized from Fp extract. But as mentioned in the UV section, the intensity of nanoparticle synthesis using BS extract is slower. On the other hand, the nanoparticle produced using Fp extract is less stable, the results of which are determined by zeta potential. Combination of Bs-Fp extracts, the speed of formation increases compared to Bs-AgNPs, and the stability also increase compared to Fp-AgNPs. As shown in Fig. 8, the size of nanoparticles synthesized from a mixture of extracts is almost equal to nanoparticles synthesized from Bs extract, at 75°C. Similar findings were reported in previous studies by Pourmortazavi et al. [38].

Figure 9 shows the effect of temperature on zeta potential. The stability of synthesized nanoparticles is dependent on the degree of aggregation. For nanoparticles synthesized using BS and FP extracts, temperature increases the rate of formation of silver nanoparticles, so increasing the numerical value of zeta potential and stability of nanoparticles. Temperature change shows a greater effect on the value of the zeta potential of Bs-AgNPs.

Based on the results of zeta potential analysis, nanoparticles synthesized from *Fumaria parviflora* extract have less stability, and nanoparticles synthesized from *Barley straw* extract have more stability. Synthesis of silver nanoparticles using a mixture of extracts (Bs-Fp) results in faster production of nanoparticles compared to Bs-AgNPs and more stable nanoparticles compared to Fp-AgNPs. It can be concluded that functional groups in *Fumaria parviflora* extract cause the faster formation of silver nanoparticles, and functional groups in *Barley straw* extract cause more stability of the synthesized silver nanoparticles. (Supporting information)

Many studies have shown that pH is a parameter that can be used to control the size of nanoparticles [39]. At high pH, silver nanoparticles with smaller sizes were obtained compared to low pH values. This difference could be related to the difference in the Ag^+ reduction rate [40]. As shown in Fig. 10, as the pH value increases, the zeta potential of nanoparticles increases, so smaller and more stable nanoparticles are formed, while the aggregation of nanoparticles decreases. As a theory, some of the functional groups in the extracts are less involved in the synthesis of silver nanoparticles and more involved in the capping and stability of nanoparticles, thereby increasing the surface charge of nanoparticles. As the PH increases, OH^- in the suspension increases, and the surface charge of the functional groups capping the nanoparticles also becomes negative, as a result, the numerical value of zeta potential and stability increases. Also, nanoparticles synthesized from the mixture of extracts, with increasing pH, the numerical value of zeta potential increased so that at pH = 12, it becomes equal to the zeta potential of nanoparticles Bs-AgNPs. As a result, using a mixture of extracts in the synthesis of nanoparticles (T = 75°C and pH = 12) leads to the faster formation of smaller and more stable nanoparticles.

3.3 Antimicrobial Activity

In recent years, antimicrobial resistance has been a common problem worldwide, as most microbial pathogens have become resistant to standard drugs in medicine to treat dreaded diseases [28]. In this study, biosynthesized silver nanoparticles were evaluated for their antimicrobial activities. The antibacterial activity of Bs extract, Fp extract, and the AgNPs synthesized using plant extracts at optimum conditions were examined on *E. coli*, as Gram-negative bacteria, and *S. aureus*, as Gram-positive bacteria, and their efficacy was shown by the inhibition zone (Fig. 11 and Table 3). The antibacterial effect of silver nanoparticles on Gram-positive and Gram-negative bacteria is different. Gram-negative bacteria (*E. coli*) showed larger inhibition zones compared to gram-positive bacteria (*S. aureus*), which may be due to the variation in cell wall composition. The cell wall of Gram-positive bacteria consists of a thick layer of peptidoglycan, while that of Gram-negative bacteria consists of a thinner layer [41]. Some differences in the antibacterial activity of Bs-AgNPs, Fp-AgNPs, and Bs-Fp-AgNPs may be related to the particle sizes or chemical composition of extracts on their surface. Smaller particles with larger surface areas show more antibacterial activity than larger particles [42, 43]. Biosynthesized nanoparticles from the mixture of extracts (Bs-Fp-AgNPs) show good antibacterial activity in Gram-positive and Gram-negative bacteria.

Table 3
The inhibition zones (mm) of AgNPs synthesized using aqueous Barley straw, Fumaria parviflora, and the mixture of aqueous extracts of Barley straw and Fumaria parviflora against E. coli and S. aureus

No.	Compounds	Zone of Inhibition (mm)	
		E. coli	S. aureus
1	Amoxicillin	19.08	18.24
2	Bs-extract	0	0
3	Fp-extract	0	0
4	Bs-AgNPs	16.02	15.23
5	Fp-AgNPs	13.13	12.47
6	Bs-Fp-AgNPs	15.38	14.67

4 Conclusion

This research presents for the first time the use of a mixture of two plant extracts for the synthesis of silver nanoparticles. Aqueous extract of *Barley straw*, *Fumaria parviflora*, and a mixture of *Barley straw* and *Fumaria parviflora* extract (1:1 v/v) were used as reducing and stabilizing agents for the green synthesis of silver nanoparticles. Various techniques were used to characterize synthesized silver nanoparticles, such as UV-Visible, FTIR, XRD, SEM/EDX and DLS. Nanoparticles obtained using these two plant species have different characteristics and biological properties. Smaller and more stable AgNPs can be obtained using Bs extract, while the nanoparticles obtained from Fp extract are formed faster. Using a

mixture of *Barley straw* and *Fumaria parviflora* extracts leads to the formation of more stable nanoparticles with better antibacterial properties.

Declarations

Conflict of interest: The authors declare that they have no conflicts of interest in the publication.

Research Involving Humans and Animals Statement: The authors declare that no humans and animals were involved in this work.

Informed Consent: All authors have seen and approved the manuscript for submission.

Authors' contributions: M. Fakharzadeh; Significant contributor to doing and writing the manuscript. S. E. Fazljoo; Prepared figures.

Availability of data and materials: The corresponding authors' data supporting this study's findings are available upon reasonable request.

Funding: This study was funded by Technical and Vocational University (TVU), Grant number 25/400/99/181

References

1. Isola, L. A., Chen, T. C., Elveny, M., Alkaim, A. F., Thangavelu, L., & Kianfar, E. (2022). Application of micro and porous materials as nano-reactors. *Reviews in Inorganic Chemistry 42*(2), 121-136. https://doi.org/10.1515/revic-2021-0007
2. Muthupandian, S., Barabadi, H., & Vahidi, H. (2021). Green nanotechnology: isolation of bioactive molecules and modified approach of biosynthesis. *Biogenic Nanoparticles Cancer Theranostics Elsevier* 101-122. https://dx.doi.org/10.1016/b978-0-12-821467-1.00005-7
3. Iravani, S., Korbekandi, H., Mirmohammadi, S., & Zolfaghari, B. (2014). Synthesis of silver nanoparticles: Chemical, physical and biological methods. *Research in Pharmaceutical Sciences 9*(6), 385-406.
4. Mohammadlou, M., Maghsoudi, H., & Jafarizadeh-Malmiri, H. (2016). A review on green silver nanoparticles based on plants: Synthesis, potential applications and eco-friendly approach. *International Food Research Journal 23*(2), 446-463.
5. Mollick, M,. Bhowmick, B., Maity, D., Mondal, D., Roy, I., & Sarkar, J. (2014). Green synthesis of silver nanoparticles-based nanofluids and investigation of their antimicrobial activities. *Microfluidics and Nanofluidics 16*(3), 541-551. https://doi.org/10.1039/C4RA07285E
6. Mihailovic, V., Katanic Stankovic, J., Selakovic, D., & Rosic, G. (2021). An overview of the beneficial role of antioxidants in the treatment of nanoparticle-induced toxicities. *Oxidative Medicine and Cellular Longevity 2021*, 1-21. https://dx.doi.org/10.1155/2021/7244677

7. Kalwar, K., & Shan, D. (2018). Antimicrobial effect of silver nanoparticles (AgNPs) and their mechanism–a mini review. *Micro & Nano Letters 13*(3), 277-280. https://dx.doi.org/10.1049/mnl.2017.0648
8. Cho, K. H., Park, J. E., Osaka, T., & Park, S. G. (2005). The study of antimicrobial activity and preservative effect of nanosilver ingredient. *Electrochimica Acta 5*(5), 956-960. https://doi.org/10.1016/j.electacta.2005.04.071
9. Yadi, M., Azizi, M., Dianat-Moghadam, H., Akbarzadeh, A., & Abyadeh, M. (2022). Antibacterial activity of green gold and silver nanoparticles using. *Bioprocess and Biosystems Engineering 45*, 1905-1917. https://doi.org/10.1007/s00449-022-02780-2
10. Barabadi, H., Vahidi, H., Damavandi Kamalim K., Rashedi, M., & Saravanan, M.(2020). Antineoplastic biogenic silver nanomaterials to combat cervical cancer: a novel approach in cancer therapeutics. *Journal of Cluster Science 31*(4), 659-672. https://doi.org/10.1007/s10876-019-01697-3
11. Cruz, D., Mostafavi, E., Vernet-Cruam A., Barabadi, H., Shah, V., & Cholula-Díaz, J. (2020). Green nanotechnology-based zinc oxide (ZnO) nanomaterials for biomedical applications: a review. *Journal of Physics: Materials 3*(3), 034005 https://dx.doi.org/10.1088/2515-7639/ab8186
12. Maťátková, O., Michailidu, J., Miškovská, A., Kolouchová, I., Masák, J., & Čejková, A. (2022). Antimicrobial properties and applications of metal nanoparticles biosynthesized by green methods. *Biotechnology advances* 58. https://doi.org/10.1016/j.biotechadv.2022.107905
13. Al-Snafi, A. (2018). Fumaria parviflora-A review. *Indo american journal of pharmaceutical sciences 5*, 1728-1738. http://doi.org/10.5281/zenodo.1210515
14. Murray, D., Jefferson, B., Jarvis, P., & Parsons, S. (2010). Inhibition of three algae species using chemicals. *Environmental Technology 31*(4), 455-466. https://doi.org/10.1080/09593331003663294
15. Rejiniemon, T., Arasu, M., Duraipandiyan, V., Ponmurugan ,K., Al-Dhabi, N., & Arokiyaraj, S. (2014). In-vitro antimicrobial, antibiofilm, cytotoxic, antifeedant and larvicidal properties of novel quinone isolated from Aegle marmelos (Linn.) Correa. *Annals of Clinical Microbiology and Antimicrobials 13*(1). https://doi.org/10.1186/s12941-014-0048-y
16. Velusamy, P., Das, J., Pachaiappan, R., Vaseeharan, B., & Pandian, K. (2015). Greener approach for synthesis of antibacterial silver nanoparticles using aqueous solution of neem gum (Azadirachta indica L.). *Industrial crops and products 66*, 103-109. https://doi.org/10.1016/j.indcrop.2014.12.042
17. Allafchian, A., Mirahmadi-Zare, S., Jalali, S., Hashemi, S., & Vahabi, M. (2016). Green synthesis of silver nanoparticles using phlomis leaf extract and investigation of their antibacterial activity. *Journal of Nanostructure in Chemistry 6*, 129-135. http://doi.10.1007/s40097-016-0187-0
18. Mittal, A., Chisti, Y., & Banerjee, U. (2013). Synthesis of metallic nanoparticles using plant extracts. *Biotechnology advances 31*, 346-356. https://doi.org/10.1016/j.biotechadv.2013.01.003
19. Srećković, N., Nedić, D., Monti, D., Mihailović, N., Stanković, J., & Dimitrijević, S. (2021). Application potential of biogenically synthesized silver nanoparticles using Lythrum salicaria L. extracts as pharmaceuticals and catalysts for organic pollutant degradation. *RSC advances 11*, 35585-35599. https://doi.org/10.1039/d1ra05570d

20. Zare-Bidaki, M., Aramjoo, H., Mizwari, Z., Mohammadparast-Tabas, P., Javanshir, R., & Mortazavi-Derazkola, S. (2022). Cytotoxicity, antifungal, antioxidant, antibacterial and photodegradation potential of silver nanoparticles mediated via Medicago sativa extract. *Arabian Journal of Chemistry 15*(16), 103842-103855. http://doi:10.1016/j.arabjc.2022.103842
21. Vanaja, M., Gnanajobitha, G., Paulkumar, K., Rajeshkumar, S., Malarkodi, C., & Annadurai, G. (2013). Phytosynthesis of silver nanoparticles by Cissus quadrangularis: influence of physicochemical factors. *Journal of Nanostructure in Chemistry 3*(1), 1-8. http://doi:10.1186/2193-8865-3-17
22. Padalia, H., Moteriya, P., & Chanda, S. (2015). Green synthesis of silver nanoparticles from marigold flower and its synergistic antimicrobial potential. *Arabian Journal of Chemistry 8*(5), 732-741. http://doi:10.1016/j.arabjc.2014.11.015
23. Kokila, T., Ramesh, P., & Geetha, D. (2015). Biosynthesis of silver nanoparticles from Cavendish banana peel extract and its antibacterial and free radical scavenging assay: a novel biological approach. *Applied Nanoscience (Switzerland) 5*, 911-920. http://doi:10.1007/s13204-015-0401-2
24. Patil, M., Palma, J., Simeon, N., Jin, X., Liu, X., & Ngabire, D. (2017). Sasa borealis leaf extract-mediated green synthesis of silver-silver chloride nanoparticles and their antibacterial and anticancer activities. *New Journal of Chemistry 41*(3), 1363-1371. http://doi:10.1039/c6nj03454c
25. Sattari, R., Khayati, G., & Hoshyar, R. (2020). Biosynthesis and Characterization of Silver Nanoparticles Capped by fumaria parviflora extract as green approach and evaluation of their cytotoxicity against human breast cancer MDA-MB-468 cell lines. *Materials Chemistry and Physics 241*, 1-28. http://doi:10.1016/j.matchemphys.2019.122438
26. Ramzan, M., Karobari, M., Heboyan, A., Noor Mohamed, R., Mustafa, M., Syed Nahid, B., & Vijay, D. (2022). Synthesis of Silver Nanoparticles from Extracts of Wild Ginger (Zingiber zerumbet) with Antibacterial Activity against Selective Multidrug Resistant Oral Bacteria. *Molecules 27*(6), 2007-2024. http://doi:10.3390/molecules27062007
27. Aglin, A., Shruthi, P., Subathra, S. (2019). Selective Toxicity of Biosynthesised Silver Nanoparticles on MCF-7 and MDA MB-231 Breast Cancer Cell Lines. *International Journal of ChemTech Research 12*(6), 7-16. http://doi:10.20902/IJCTR.2019.120602
28. Khan, M., Karuppiah, P., Alkhathlan, H., Kuniyil, M., Khan, M., & Adil, S. (2022). Green Synthesis of Silver Nanoparticles Using Juniperus procera Extract: Their Characterization, and Biological Activity. *crystals 12*(3), 1-13. https://doi.org/10.3390/cryst12030420
29. Hanachi, P., Gharari, Z., Sadeghinia, H., & Walker ,T. (2022). Synthesis of bioactive silver nanoparticles with eco-friendly processes using Heracleum persicum stem extract and evaluation of their antioxidant, antibacterial, anticancer and apoptotic potential. *Journal of Molecular Structure 1265*, 270-286. https://doi.org/10.1016/j.molstruc.2022.133325
30. Nafeesa, K., Jahirul Ahmed, M., & Sardar, M. (2017). Biotechnological Applications of Green Synthesized Silver Nanoparticles. *Journal of Nanosciences: Current Research 2*(1), 2572-0813. http://doi:10.4172/2572-0813.1000107

31. Verma, A., & Mehata, M., (2016). Controllable synthesis of silver nanoparticles using Neem leaves and their antimicrobial activity. *Journal of Radiation Research and Applied Sciences 9*(1), 109-115. http://doi:10.1016/j.jrras.2015.11.001
32. Rakib-Uz-Zaman, S., Apu, E., Muntasir, M., Mowna, S., Khanom, M., & Jahan, S. (2022). Biosynthesis of Silver Nanoparticles from Cymbopogon citratus Leaf Extract and Evaluation of Their Antimicrobial Properties. *Challenges 13*(1), 1-18. https://doi.org/10.3390/challe13010018
33. Song, J., & Kim, B. (2009). Rapid biological synthesis of silver nanoparticles using plant leaf extracts. *Bioprocess and Biosystems Engineering 32*(1), 79-84. http://doi:10.1007/s00449-008-0224-6
34. Khane, Y., Benouis, K., Albukhaty, S., Sulaiman, G., Abomughaid, M., & Al Ali, A. (2022). Green Synthesis of Silver Nanoparticles Using Aqueous Citrus limon Zest Extract: Characterization and Evaluation of Their Antioxidant and Antimicrobial Properties. *Nanomaterials 12*(12), 1-20. http://doi:10.3390/nano12122013
35. Mihailovi´c, V., Srećković, N., Nedić, Z., Dimitrijević, S., Matić, M., & Obradović, A. (2023). Green Synthesis of Silver Nanoparticles Using Salvia verticillata and Filipendula ulmaria Extracts: Optimization of Synthesis, Biological Activities, and Catalytic Properties. *Molecules 28*(2), 808-831. https://doi.org/10.3390/molecules28020808
36. Rajeshkumar, S., & Bharath, L. (2017). Mechanism of plant-mediated synthesis of silver nanoparticles – A review on biomolecules involved, characterisation and antibacterial activity. *Chemico-Biological Interactions 27*, 219-227. https://doi.org/10.1016/j.cbi.2017.06.019
37. Saied, E., Eid, A., Hassan, S. D., Salem, S., Radwan A, Halawa, M., & Saleh, F. (2021). The catalytic activity of biosynthesized magnesium oxide nanoparticles (MgO-nps) for inhibiting the growth of pathogenic microbes, tanning effluent treatment, and chromium ion removal. *Catalysts 11*(7), 821-840. https://doi.org/10.3390/catal11070821
38. Pourmortazavi, S., Taghdiri, M., Makari, V., & RahimiNasrabadi, M. (2015). Procedure optimization for green synthesis of silver nanoparticles by aqueous. *Spectrochimica Acta Part A: Molecular and Biomolecular Spectroscopy 136*, 1249-1254. https://doi.org/10.1016/j.saa.2014.10.010
39. Anigol, L., Charantimath, J., & Gurubasavaraj, P. (2017). Effect of concentration and pH on the size of silver nanoparticles synthesized by green chemistry. *Org. Med. Chem. Int. J.3*(5), 1-5. http://doi.org/10.19080/omcij.2017.03.555622
40. Gontijo, L., Raphael, E., Ferrari, D., & Ferrari, J. (2020). pH effect on the synthesis of different size silver nanoparticles evaluated by dls and their size-dependent antimicrobial activity. *Revista Materia 25*(4). https://doi.org/10.1590/S1517-707620200004.1145
41. Rizzello, L., & Pier Paolo, P. (2014). Nanosilver-based antibacterial drugs and devices: Mechanisms, methodological drawbacks, and guidelines. *Chemical Society Review 43*(5), 1501-1518. http://doi:10.1039/c3cs60218d
42. Kim, J., Kuk, E., Yu, K., Kim, J. H., Park, S., Lee, H., & Park, Y. (2007). Antimicrobial effects of silver nanoparticles. *Nanomedicine: Nanotechnology, biology and medicine 3*(1), 95-101. https://doi.org/10.1016/j.nano.2006.12.001

43. Macovei, I., Luca, S., Skalicka-Woźniak, K., Sacarescu, L., Pascariu, P., Ghilan, A., & Doroftei, F. (2022). Phyto-functionalized silver nanoparticles derived from conifer bark extracts and evaluation of their antimicrobial and cytogenotoxic effects. *Molecules27*(1), 217. https://doi.org/10.3390/molecules27010217

44. Vanaja, M., Gnanajobitha, G., Paulkumar, K., Rajeshkumar, S., Malarkodi, C., & Annadurai, G. (2013). Phytosynthesis of silver nanoparticles by Cissus quadrangularis: influence of physicochemical factors. *Journal of Nanostructure in Chemistry 3*. https://doi.org/10.1186/2193-8865-3-17

Figures

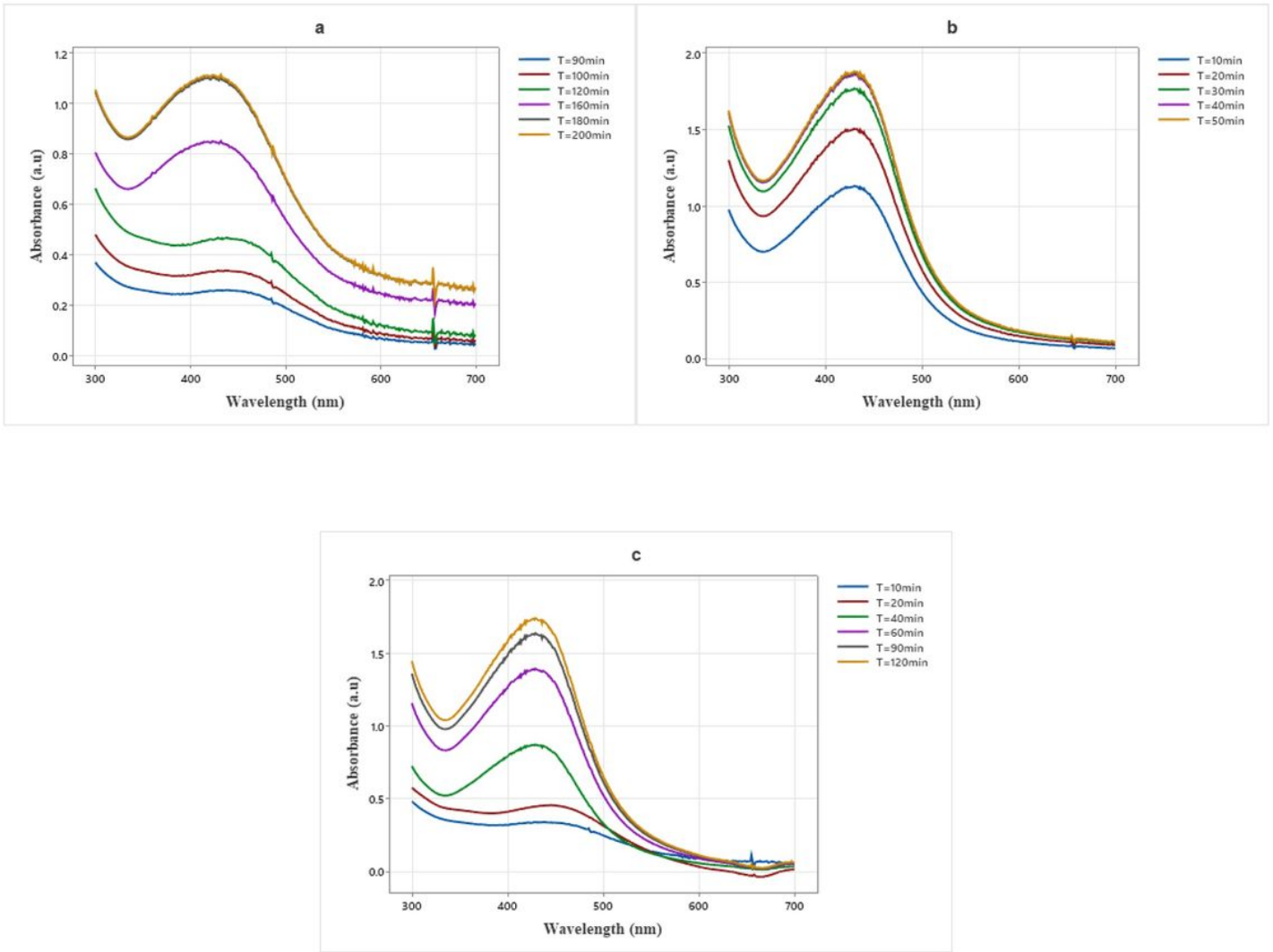


Figure 1

Effect of reaction time T=25 °C, PH=12 a) Bs-AgNPs b) Fp-AgNPs c) Bs-Fp-AgNPs

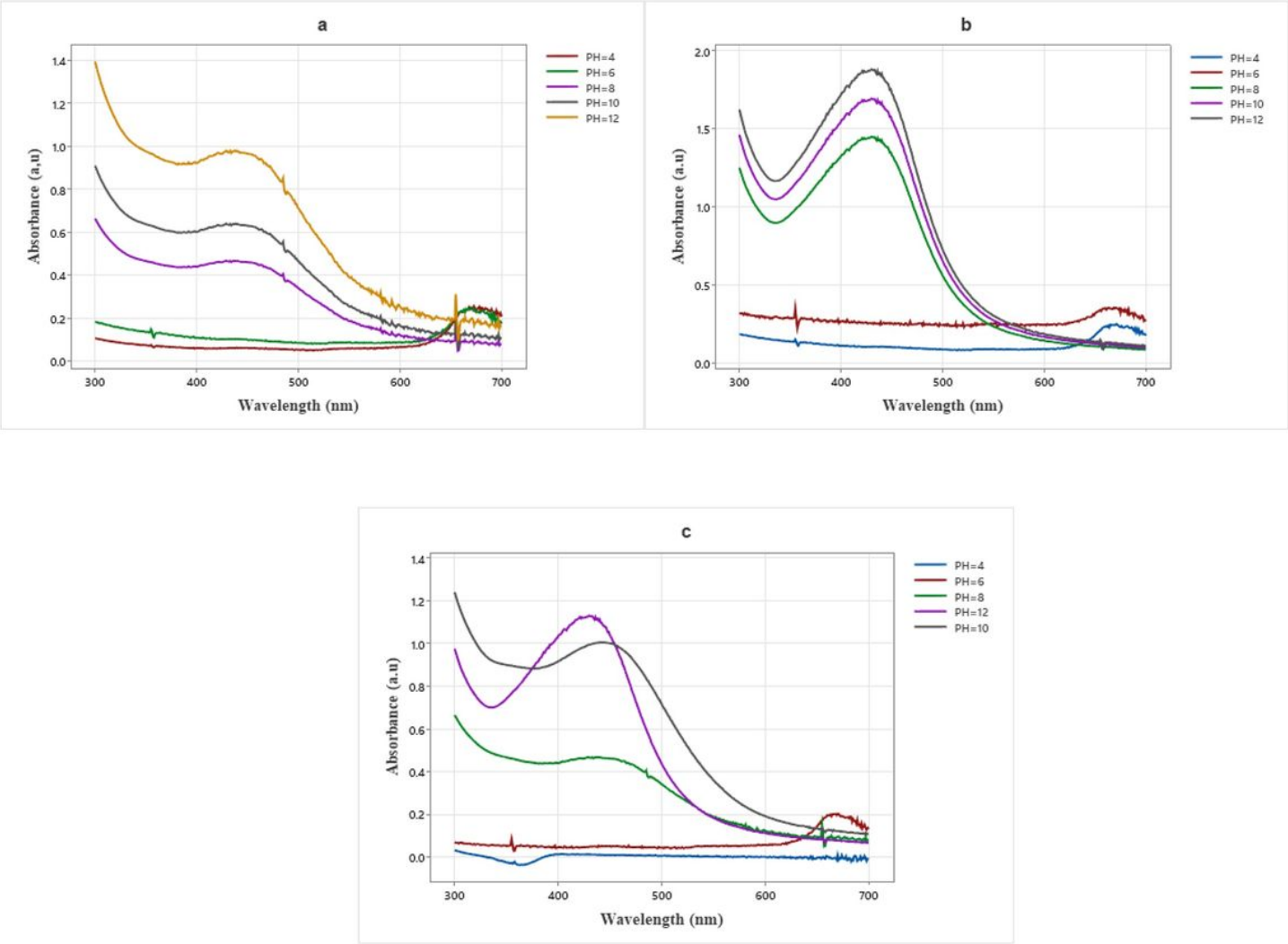


Figure 2

Effect of PH T=25 °C, a) Bs-AgNPs, reaction time=180 min b) Fp- AgNPs, reaction time=40 min c) Bs-Fp-AgNPs, reaction time=90 min

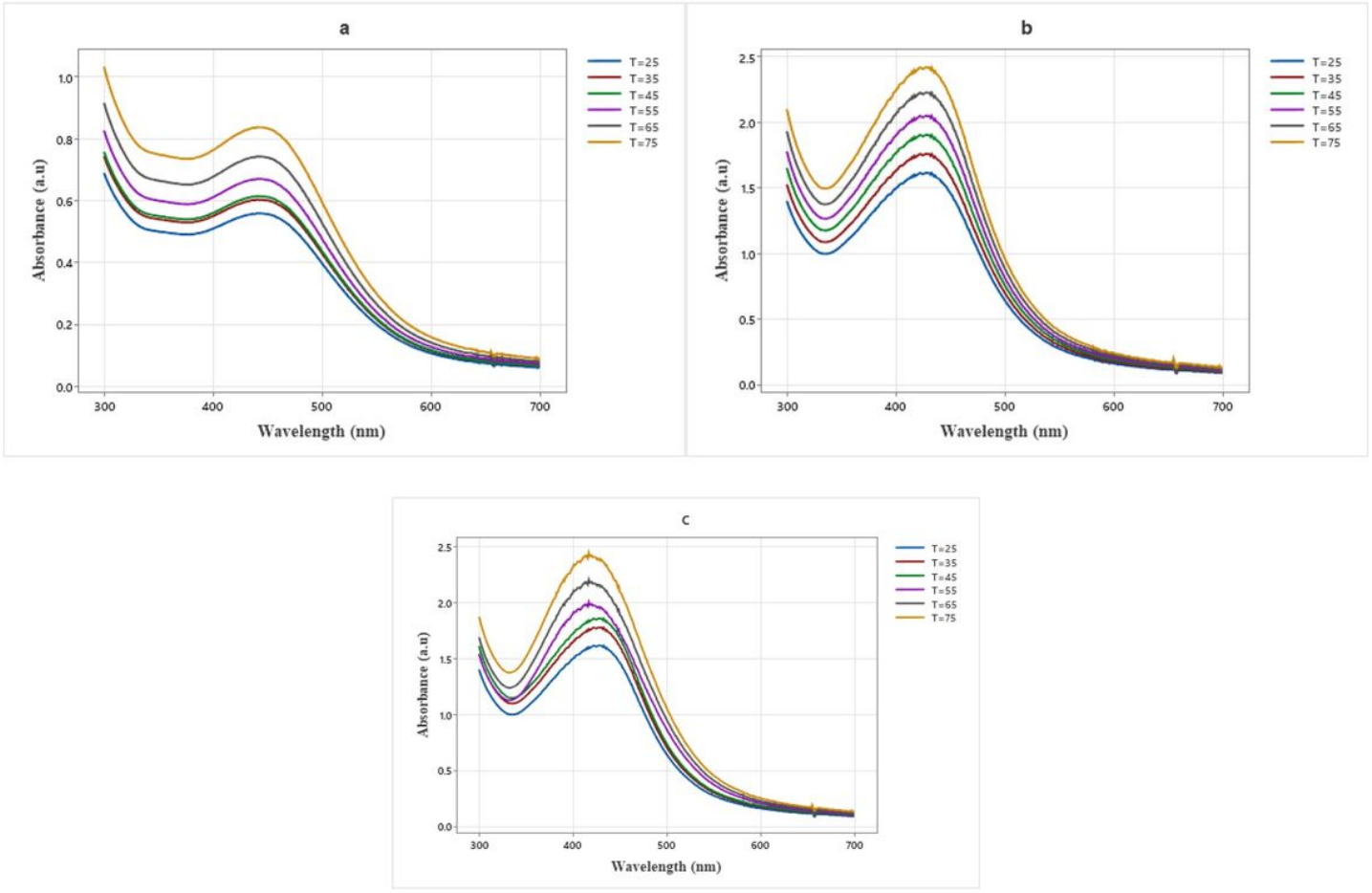


Figure 3

Effect of temperature, PH=12 , a) Bs-AgNPs, reaction time=180 min b) Fp- AgNPs, reaction time=40 min c) Bs-Fp-AgNPs, reaction time=90 min

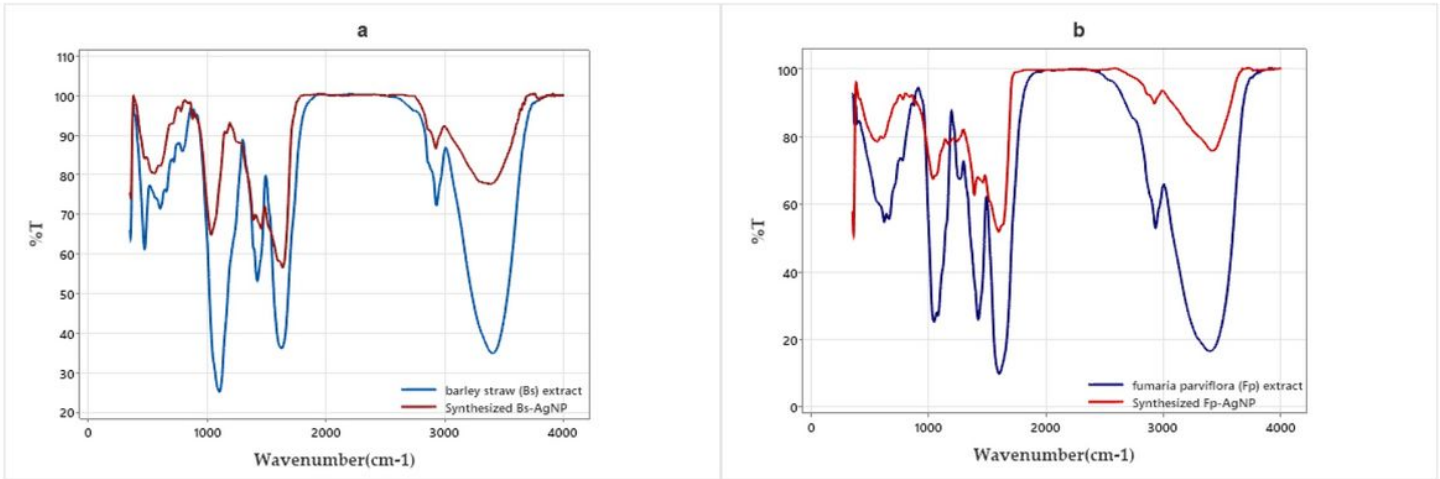


Figure 4

FTIR spectra of a) Bs extract and Synthesized Bs-AgNPs b) Fp extract and Synthesized Fp-AgNPs

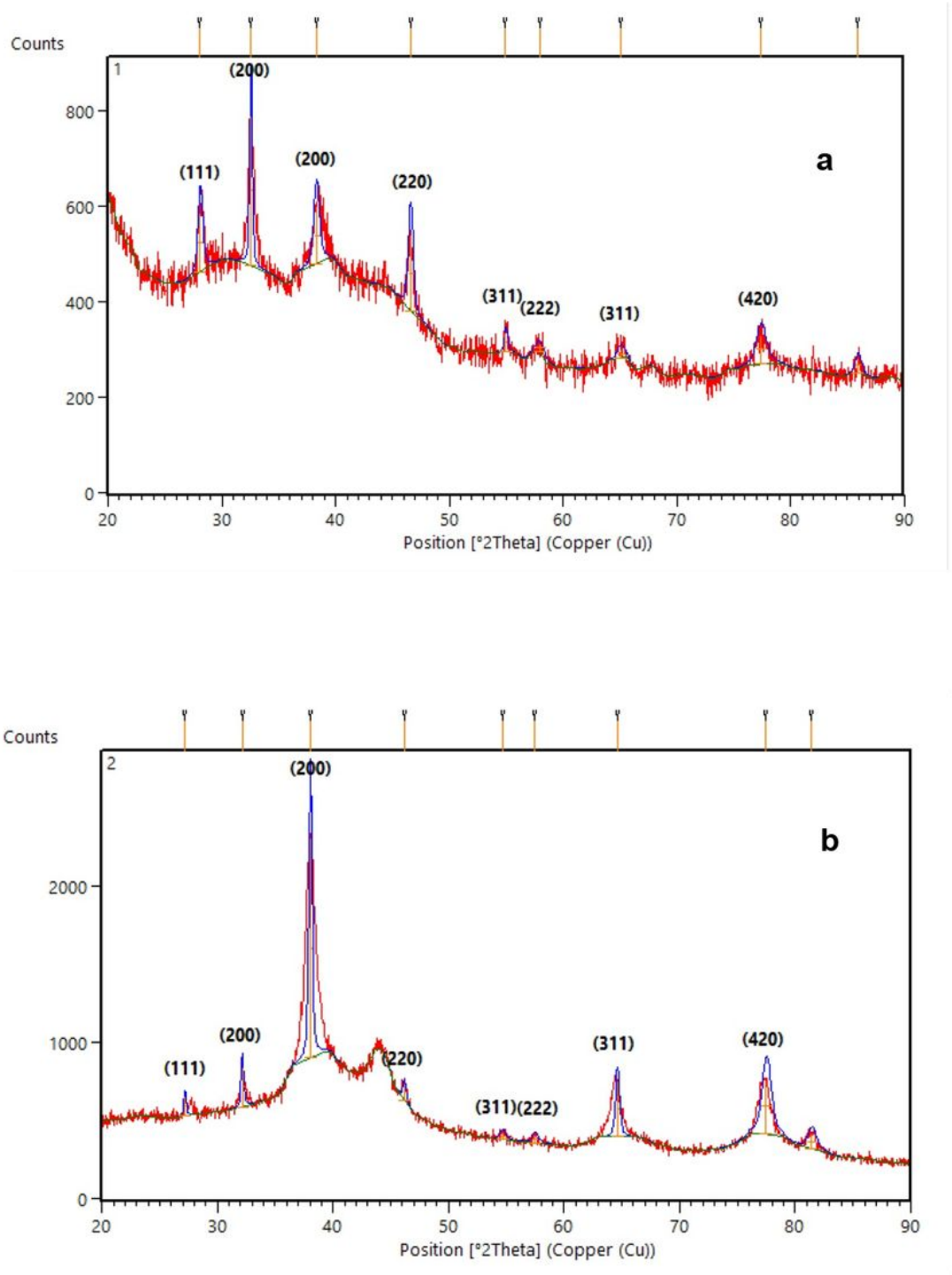


Figure 5

XRD pattern of synthesized a) Bs-AgNP b) Fp-AgNP

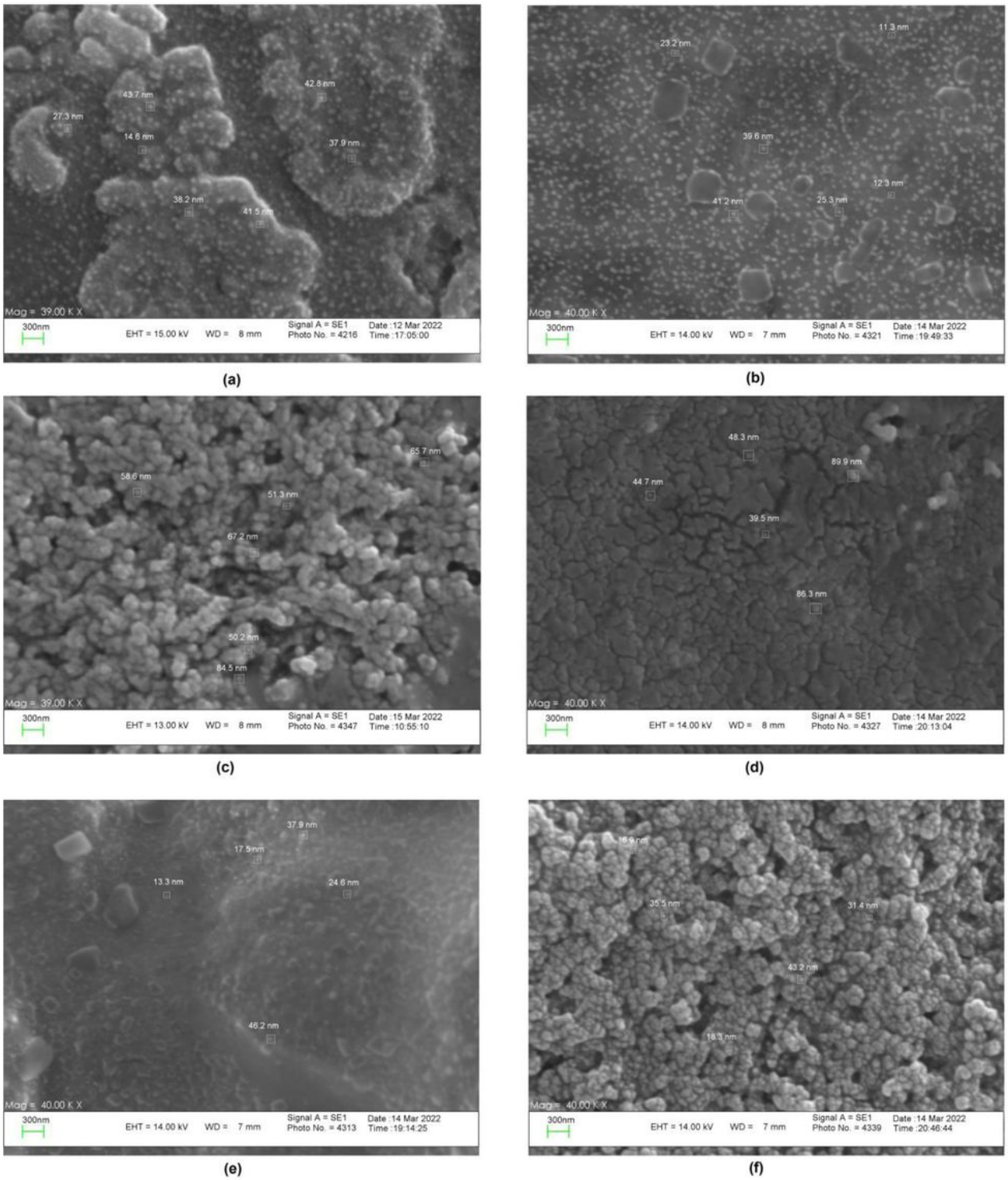


Figure 6

SEM image of biosynthesized NPs a) Bs-AgNPs, 25°C b) Bs-AgNPs, 75°C c) Fp-AgNPs, 25°C d) Fp-AgNPs, 75°C e) Bs-Fp-AgNPs, 25°C f) Bs-Fp-AgNPs, 75°C

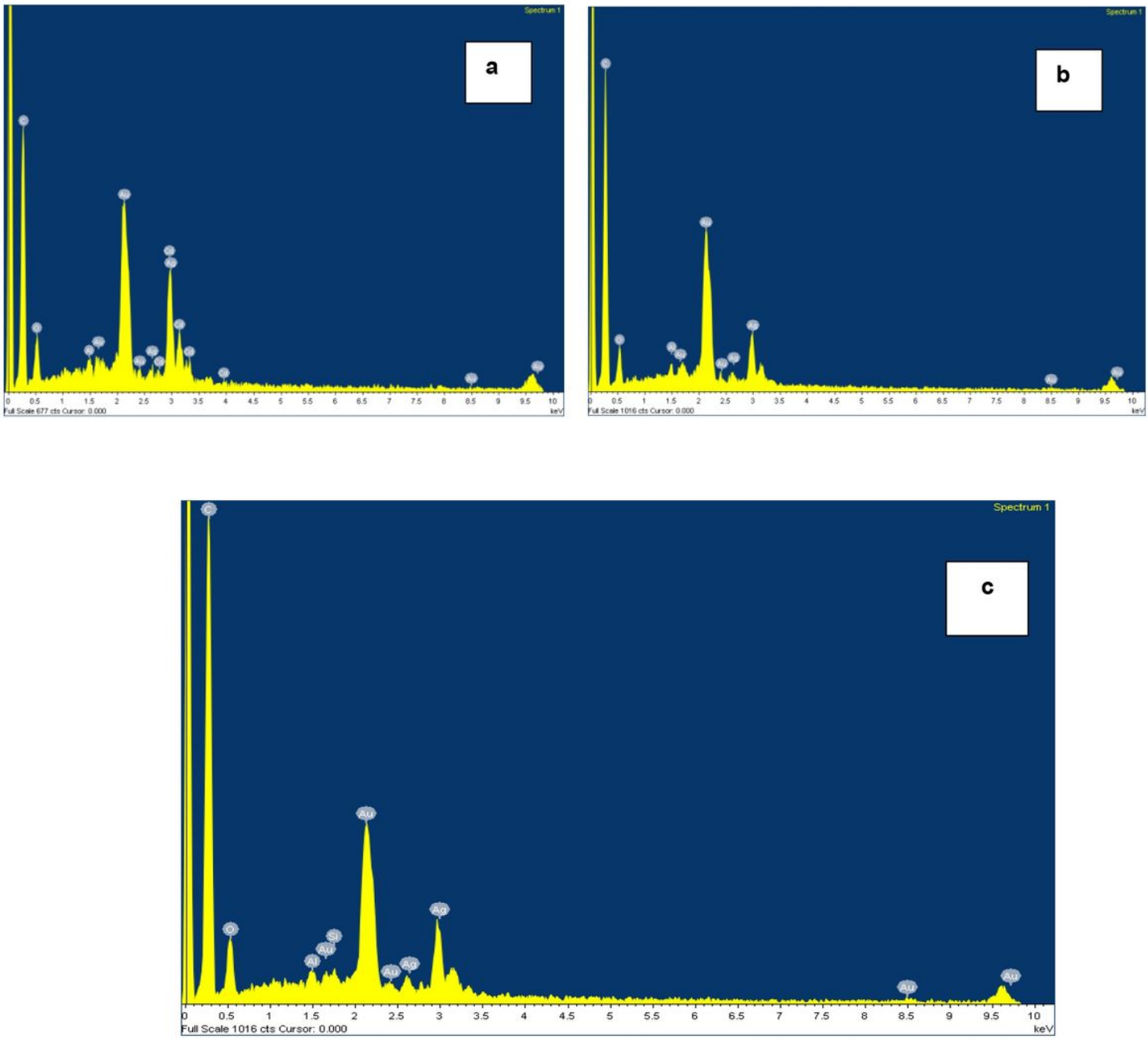


Figure 7

EDX spectra of AgNPs synthesized from a) Bs-AgNPs b) Fp-AgNPs c) Bs-Fp-AgNPs

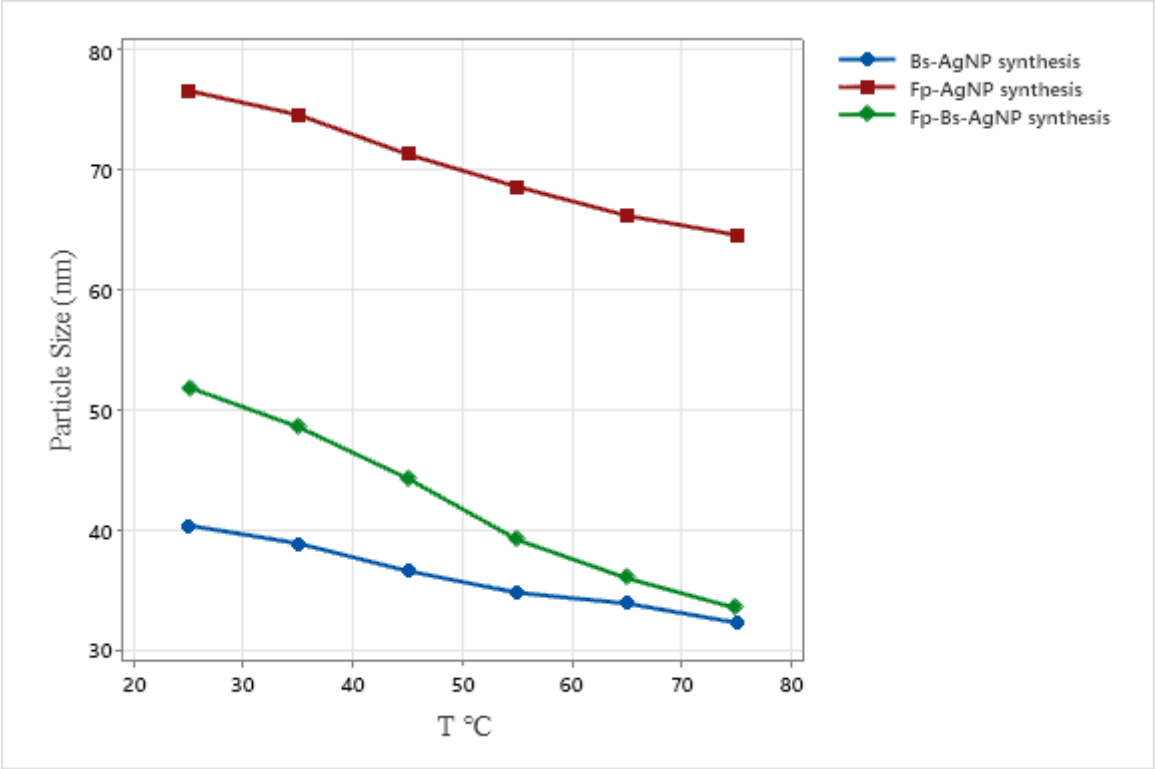


Figure 8

Effect of Temperature on Particle Size

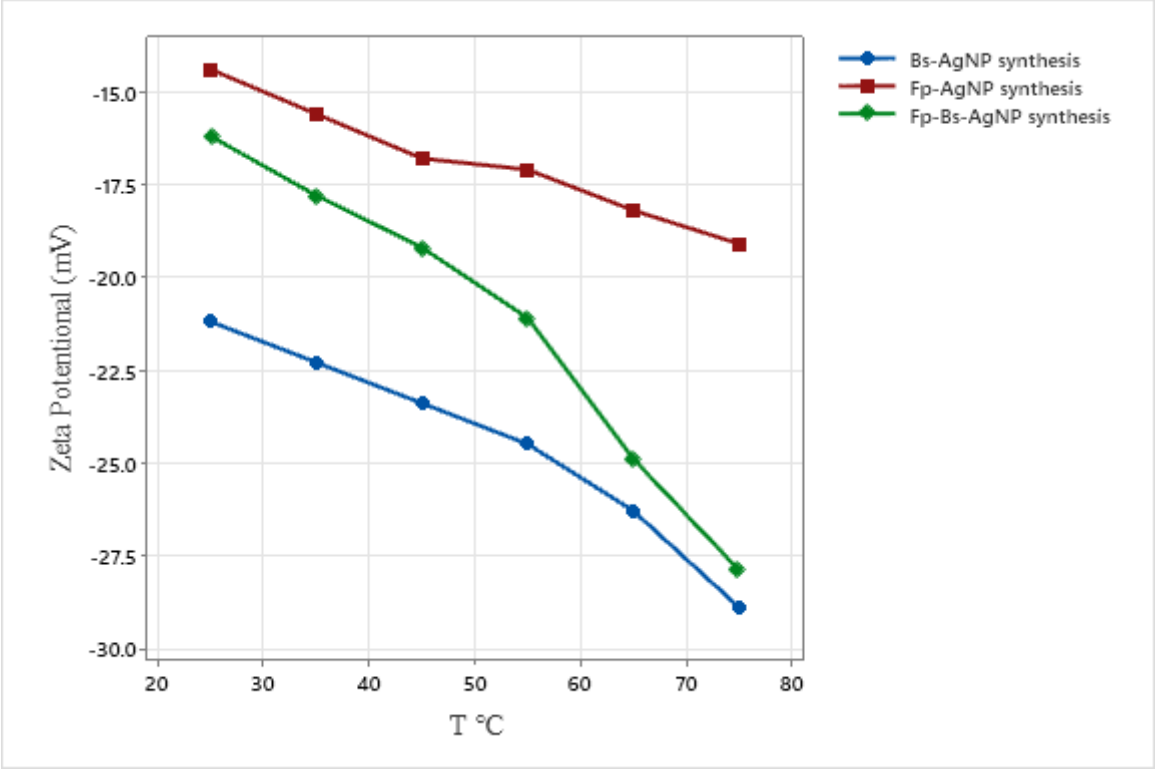


Figure 9

Effect of Temperature on Zeta Potential

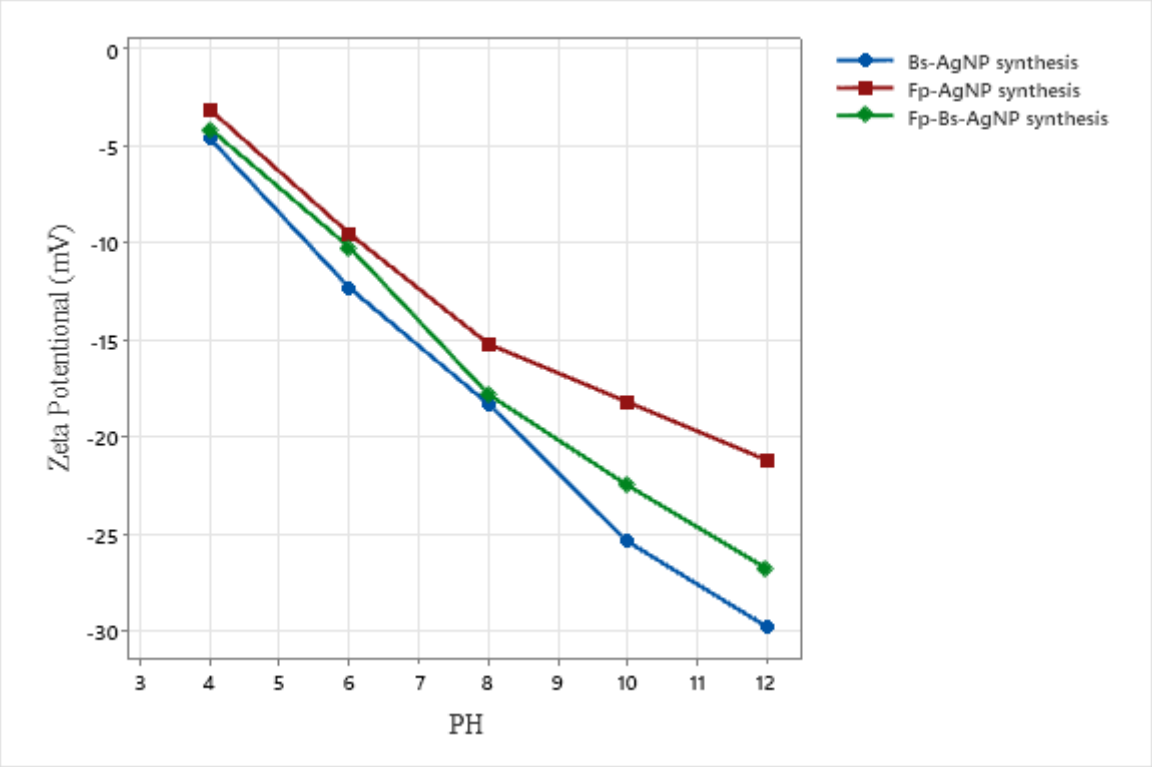


Figure 10

Effect of PH on Zeta Potential



Figure 11

Antibacterial activity of 1. Amoxicillin, 2. Bs extract, 3. Fp extract, 4. Bs-AgNPs, 5. Fp-AgNPs, 6. Bs-Fp-AgNPs against Gram-positive (*Staphylococcus aureus*) and Gram-negative (*Escherichia coli*)

Supplementary Files

This is a list of supplementary files associated with this preprint. Click to download.

- Suplimentalfile.pdf